Published in final edited form as:
Chembiochem. 2011 November 4; 12(16): 2441–2447. doi:10.1002/cbic.201100469.

Cell Targeting with Hybrid Qβ Virus-Like Particles Displaying Epidermal Growth Factor

Dr. Jonathan K. Pokorski, **Marisa L. Hovlid**, and **Prof. M.G. Finn**
Department of Chemistry, The Scripps Research Institute, 10550 N. Torrey Pines Road, La Jolla, CA 92037 (USA), Fax: (+1) 858-784-8850

M.G. Finn: mgfinn@scripps.edu

Abstract

Structurally uniform protein nanoparticles derived from the self-assembly of viral capsid proteins are attractive platforms for the multivalent display of cell-targeting motifs for use in nanomedicine. Virus-based nanoparticles are of particular interest because the scaffold can be manipulated both genetically and chemically to simultaneously display targeting groups and carry a functional payload. Here, we displayed the human epidermal growth factor (EGF) on the exterior surface of bacteriophage Qβ as a C-terminal genetic fusion to the Qβ capsid protein. The co-assembly of wild-type Qβ and EGF-modified subunits resulted in structurally homogeneous nanoparticles displaying between 5 and 12 copies of EGF on their exterior surface. The particles were found to be amenable to bioconjugation via standard methods as well as the high-fidelity copper catalyzed azide-alkyne cycloaddition reaction (CuAAC). Such chemical derivatization did not impair the ability of the particles to specifically interact with the EGF receptor. Additionally, the particle-displayed EGF remained biologically active promoting auto-phosphorylation of the EGF receptor and apoptosis of A431 cells. These results suggest that hybrid Qβ-EGF nanoparticles could be useful vehicles for targeted delivery of imaging and/or therapeutic agents.

Keywords

epidermal growth factor; nanoparticles; viruses; cell targeting; bioconjugation; multivalency

Introduction

New methods for delivering drugs specifically to tissues of interest are becoming increasingly desirable as we expand our understanding of the hallmarks of certain diseases such as cancer. Platforms that deliver chemotherapeutics selectively to tumor cells would have the advantage of increased efficacy and a decrease in debilitating off-target effects. Of particular interest are nanoscale platforms that integrate several functions into a single therapeutic vehicle, such as targeting motifs to direct particles to destinations of choice and imaging or therapeutic agents to visualize their locale or to achieve a desired outcome.[1] Nanoparticles provide a relatively large surface area for derivatization, allowing the display of multiple copies of a targeting ligand on each particle, along with cargo molecules attached to the surface or packaged within. A variety of nanoscale platforms are in development that have been engineered to deliver payloads to cellular environments in which differential expression of cell surface receptors is a hallmark of the disease state. Examples include nanoparticles derived from viruses and virus like particles (VLPs),[2]

Correspondence to: M.G. Finn, mgfinn@scripps.edu.

Supporting information for this article is available on the WWW under http://www.chembiochem.org or from the author.

polymers,[3] inorganic colloids,[4] and mammalian protein cage complexes such as the vault[5] and heat shock proteins.[6]

A popular molecular target in cancer research is the epidermal growth factor receptor (EGFR), which is overexpressed on a variety of malignant cell types.[7] Activation of EGFR initiates signaling events that result in a wide variety of processes ranging from chemotaxis and proliferation to apoptosis.[8] Strategies to address malignancies that overexpress EGFR include the use of small molecules that act directly on the receptor,[9] monoclonal antibody-based therapy,[10] and receptor targeted formulations to deliver cytotoxic agents.[11] Two recent examples appear in the literature detailing genetic[5b] or chemical fusion[12] of the epidermal growth factor (EGF) to protein nanoparticles for receptor-specific binding.

We describe here the development and use of a variant of the *Levivirus* bacteriophage Qβ capsid protein (CP) that binds EGFR tightly. When expressed recombinantly in *E. coli*, 180 copies of the Qβ capsid protein assemble into icosahedra of T=3 symmetry.[13] The resulting particle is approximately 28 nm in diameter and, like other members of its family,[14] is stable to temperatures in excess of 70°C as well as to organic co-solvents.[15] Qβ VLPs are particularly advantageous because of their high production yields and tolerance toward extensive genetic and chemical modification. We have recently reported that proteinaceous ligands can be displayed on the exterior surface of Qβ capsids through a simple two-plasmid co-expression system, in which one plasmid coding for a truncated (133 amino acid) version of the native coat protein (pET28CP) and a second coding for that protein plus a polypeptide extension at the C-terminus (pCCP8Fusion) are expressed simultaneously (Figure 1).[16] Each C-terminus is found on the exterior surface of the capsid.[13] Proteins have been genetically encoded into protein nanoparticle sequences for the surface display of protein antigens on flock house virus[17] and bacteriophage MS2 VLPs,[18] and for display of ligand- or antibody-binding domains on baculovirus,[19] hepatitis B capsids,[20] and vault proteins.[5b] We draw a practical and functional distinction between these kinds of cases, which emphasize the direct use of the functionalized particles, and phage display of protein domains on the terminus of M13 virions for the purpose of selecting tight-binding sequences.

The number of extensions per particle in our Qβ system varies from 4 to approximately 40 and is typically inversely dependent on the size and expression level of the incorporated extension. To show that this method can be used to program the binding and biochemical effects of these particles, we describe here the production of Qβ VLPs encoded to display EGF and explore their interactions with cells over-expressing their cognate receptor.

Results and Discussion

VLP cloning and expression

The epidermal growth factor (EGF) is a 53-amino acid polypeptide that mediates cellular proliferation and has previously been expressed and purified from *E. coli* in an active form.[21] Initially, a codon-optimized EGF gene, including appropriate cloning sites at both termini for insertion into the pCDFCP8 backbone was prepared by PCR-based total gene synthesis.[22] Standard molecular cloning techniques were used to introduce this fragment, preceded by a short hydrophilic spacer peptide, at the C-terminus of the CP sequence to yield pCCP8EGF. The spacer peptide was designed to give the EGF domain some flexibility in presentation from the capsid surface and to allow independent folding of both domains into their functional forms. Transformation of this plasmid along with the standard pET28CP plasmid into competent BL21(DE3) cells followed by IPTG-induced protein expression gave high yields of particles isolated and purified by standard techniques.[16a, 23] The resultant VLPs exhibited a hydrodynamic radius (14.8 nm) and size-exclusion

chromatography elution profile characteristic of unmodified Qβ particles (Figure 1). Transmission electron microscopy also showed normal particle morphology, indistinguishable from wild-type particles (data not shown). Microfluidic electrophoretic analysis (Agilent Bioanalyzer) of the purified VLPs showed two protein bands corresponding to wild-type and EGF-fusion capsid proteins. Their molar ratio, which defines the average number of EGF-bearing subunits in the particle, was determined by the relative intensities of these bands, corrected for their respective molecular weights.[16a, 23] [16a, 23][16a, 23][16a, 19] In this way, typical particle preparations varied between an average of 5 to 12 EGF domains per VLP (designated $Q\beta(EGF)_n$, where n = the average number of capsid proteins bearing the EGF domain in each particle).

Several empirically observed factors contributed to increased particle yields and fusion incorporation ratios. For instance, optimization of expression media is critical for increasing fusion expression and thus incorporation numbers. In a previous report, the incorporation of Z-domains into Qβ was most effective when expressions were carried out in minimal expression media (MEM).[16a] However, the expression level of the CP-EGF fusion gene was suppressed in MEM by approximately 50% relative to that in super optimal broth (SOB). This resulted in a significant decrease in fusion incorporation, with MEM preparations yielding particles bearing between 1 and 3 fusions. Additionally, yields were highly dependent on buffer selection in the initial stages of the virus purification procedure (cell lysis and protein precipitation steps), due presumably to the tendency of EGF domains to aggregate with each other. Our usual protocol is performed in phosphate-buffered saline (PBS) to simplify downstream chemical modification via NHS chemistry. In this case, particle aggregates were formed that could not be purified to homogeneity. By substituting tris-buffered saline (TBS) for PBS during the early stages of purification, virtually all aggregation problems were eliminated, for reasons that we do not understand. Purified particles could then be resuspended in PBS to yield a stable homogeneous particle population. The final yields of purified particles were typically 25 mg protein per liter of culture, which is moderate for engineered Qβ VLPs.

Bioconjugation for dye labeling

AlexaFluor488[24] was conjugated to both EGF-displaying and wild type particles to allow for their visualization in cellular binding and uptake studies. A two-step procedure was employed, relying on the powerful copper-catalyzed azide-alkyne cycloaddition (CuAAC) reaction to maximize efficiency when using the expensive fluorophore (Figure 2).[25] In this case, the relatively “light” loading of the EGF domain on the particle proved to be advantageous. Although several examples exist where lysine modification has only a modest impact on biological function,[26] it was unclear if this would be the case for our system.[27] Thus, we preferred to minimize acylation of the EGF lysine residues in the initial reaction step where the azide was installed. Each of the 180 Qβ subunits exposes four amine groups to the outer surface, presenting a total of 720 reactive sites, compared to a total of two amine groups per displayed EGF motif (10-24 additional lysines per particle). Even assuming all of the latter lysines are accessible to acylating agents, the use of non-forcing reaction conditions should leave most amine groups on the EGF ligand untouched, due to the vast excess of lysines associated with the capsid protein. We presumed that this would allow the displayed EGF to function normally in binding its receptor.

Following acylation, an AlexaFluor488 derivative bearing a pendant alkyne was introduced using the CuAAC reaction. The resulting conjugates were found to have approximately 20 dyes per particle as determined by comparing total protein concentration (Bradford assay) to the concentration of AlexaFluor488 determined by UV-Vis spectroscopy. Confocal microscopy and flow cytometry studies described below showed that the resulting particles

(**5**) retained their ability to specifically interact with EGFR positive cells, suggesting that neither the acylation nor the 'click' step block a substantial number of the EGF-EGFR binding sites.

Cell binding experiments

The epidermoid carcinoma A431 cell line is an established overexpressor of the EGF receptor,[28] and has frequently been used to validate EGFR targeting.[5b, 11a, 29] Figure 3 shows representative confocal fluorescence microscopy images showing that Qβ$(EGF)_{11}(A488)_{20}$ particles (**5**) bound these cells strongly at 4°C (Figure 3B), while dye-labeled particles lacking the EGF domain bound only weakly (Figures 3A). Additionally, at 37 °C Qβ$(EGF)_{11}(A488)_{20}$ were internalized in a punctate pattern consistent with the expected receptor-mediated endocytosis pathway (Figure 3E,F), while dye-labeled particles lacking the EGF domain did not internalize (Figure 3D). The presence of excess recombinant human EGF (rhEGF) protein inhibited binding of the EGF-bearing particles at 4°C (Figure 3C), showing that the particle interactions were dominated by the EGF-EGFR interaction rather than nonspecific associations between the capsid protein and the cell surface.

The binding interaction of Qβ-EGF with its cognate receptor was further probed using flow cytometry. A431 cells were incubated with Qβ$(EGF)_{11}(A488)_{20}$, Qβ$(A488)_{20}$, or Qβ$(EGF)_{11}(A488)_{20}$ plus excess rhEGF for one hour at 37°C (Figure 4). The Qβ$(A488)_{20}$ particles displayed virtually no nonspecific binding to cells, exhibiting a fluorescence intensity comparable to the background signals produced by cells alone. Cells incubated with the Qβ$(EGF)_{11}(A488)_{20}$ construct, however, produced a fluorescence signal more than 15 times greater than both background and Qβ$(A488)_{20}$. Competition experiments showed a drop-off in particle binding, evidenced by decreased fluorescence as increasing amounts of soluble EGF were titrated against a fixed concentration of Qβ$(EGF)_{11}(A488)_{20}$. The presence of 100 fold molar excess rhEGF relative to particle-displayed EGF was sufficient to abolish Qβ$(EGF)_{11}(A488)_{20}$ binding, reducing fluorescence signal to background levels.

EGFR activation assays

The biological effects of the interaction of EGF with the EGF receptor are well understood. Receptor binding rapidly leads to dimerization and is accompanied by several autophosphorylation events,[8] which trigger signalling cascades through phosphotyrosine binding proteins. To verify that Qβ-displayed EGF mediates a similar response, we measured phosphorylation at Y1173[30] using a whole-cell ELISA assay as an indicator of receptor activation (Figure 5). At the same total protein concentration, both soluble rhEGF and Qβ$(EGF)_6$ gave an increase of approximately 80% in receptor phosphorylation. Particles lacking the EGF domain showed no such increase in phosphorylation, indeed they produced an unexpected decrease in phosphorylation at high concentrations (Figure 5A). These results suggest that the necessary restriction of the N-terminus of the growth factor by attaching it to the VLP had little effect on biological activity. Unfortunately, no benefits due to polyvalent effects were observed.

While EGF is a potent mitogen at low concentrations, at high concentrations it has the opposite biological effect, promoting apoptosis in A431 cells.[31] An evaluation of cytotoxicity is shown in Figure 5B. Here, too, rhEGF and Qβ$(EGF)_6$ had similar effects on cell viability, resulting in approximately 60% cell-death after 72 h in the presence of high nanomolar concentrations of either form of EGF. After such treatment, the cells treated with both EGF formulations exhibited a condensed morphology consistent with that previously observed upon treatment with high concentrations of EGF.[32] Particles lacking the EGF extensions had no significant effect on A431 viability.

Conclusion

This report detailed the construction of genetically encoded hybrid virus-like particles derived from bacteriophage Qβ that display functional copies of EGF. This type of genetically encoded addressability is versatile and modular, providing access to essentially any peptide or protein that can be expressed in *E. coli*., and the cost of production is little more than the cost of media. As we have shown, Qβ is amenable to conjugation chemistry, allowing us to deliver imaging or therapeutic molecules to cells of interest. In the case studied here, a relatively small fraction of incorporated fusion proteins provided effective cell binding and internalization, presumably because of the high affinity of the EGF-EGFR interaction. This leaves most of the exterior surface of the nanoparticle for further chemical derivatization. These results offer a critical component in the quest to make an affordable and scalable nanoparticle platform that can incorporate a diverse array of function into a single particle.

Experimental Section

Cloning of pCCP8EGF

A pCDFCP8-fusion plasmid was previously available in our lab, with a multiple cloning site immediately downstream of the CP gene containing NcoI and XhoI sites.[16a] The sequence for each individual gene to be cloned, including appropriate restriction sites, was input into GeneDesign 2.0 and codon optimized for expression in *E. Coli*.[22] The primers generated by the gene design program were used for a PCR-based total gene synthesis. An equimolar primer mix was used as the template for the assembly reaction, where the final total primer concentration in the PCR reaction was 2 μM. After 55 thermal cycles, the product was run on a gel and a band of the approximate size desired was excised and extracted. The resultant DNA was diluted 10 fold and used as the template in a PCR reaction, where the forward and reverse primers corresponded to the two terminal primers from the assembly reaction. The amplified DNA product was agarose gel purified, excised from the gel, and extracted. The extracted DNA and pCCP8-fusion plasmid were both digested with NcoI and XhoI. The pCDFCP8 vector was isolated from the insert by agarose gel electrophoresis and the EGF gene was isolated via spin column purification. The desired gene was ligated into the pCDFCP8 backbone using T4 DNA ligase to form pCCP8EGF.

Protein Expression and Purification

Competent BL21(DE3) *E. coli* cells were simultaneously transformed with pET28CP/pCCP8EGF and plated onto SOB agar media containing appropriate antibiotics. The following day, well-isolated colonies were picked from plates into 25 mL of autoclaved selective super optimal broth (SOB) media and grown to saturation overnight at 37 °C. The following morning the cultures were diluted into 500 mL of freshly prepared selective SOB. Culture growth was monitored by following optical density at 600 nm (OD_{600}). When the OD_{600} of the cultures reached approximately 0.9 (mid-log phase), protein expression was induced with the addition of 500 μL of 1M IPTG, giving a final IPTG concentration of 1 mM. Shaking was continued at 37 °C for an additional 4 hours, at which point cells were collected by centrifugation in a JA-17 rotor at 14,000 rpm for 10 minutes. The supernatant was decanted and the cell pellet was frozen at -20 °C overnight. The following morning, cells were resuspended in ~50 mL of 1x TBS (pH 7.4). The buffer used for the original resuspension continued to be used for subsequent steps of particle preparation. Samples were chilled on ice and then sonicated with a probe sonicator (10 minutes total sonication time, in cycles of 5 seconds on and 5 seconds off) in an ice bath to lyse cell membranes. The resulting cell debris was pelleted in a JA-17 rotor at 14,000 rpm for 10 minutes and the supernatant was decanted away from the pellets and collected. The VLPs were precipitated

from the resulting supernatant by the addition of 10 % w/v PEG8000 on ice for a minimum of 30 minutes. The precipitated fraction was isolated from the supernatant by centrifugation in a JA-17 rotor for 10 minutes at 14,000 rpm. The pellet was re-dissolved in the appropriate buffer (~15 mL) and extracted with a 1:1 v/v solution of *n*-BuOH:$CHCl_3$ to remove excess lipid and aggregated VLPs. The aqueous fraction was collected following centrifugation (14,000 rpm, 5 min). Virus-like particles were purified on 10-40% sucrose velocity gradients in an SW28 rotor at 28,000 rpm for 3.5 hours. Approximately 4 mL was pulled from each gradient and subsequently pelleted in an ultracentrifuge (50.2Ti rotor, 48K, minimum 2 hours). The purified protein was dissolved in phosphate-buffered saline (PBS) and characterized. VLP purity was assessed using FPLC size exclusion chromatography with Superose 6 gel and monitored by eluent absorbance at 260 nm and 280 nm. The size of purified particles was determined by dynamic light scattering using a Wyatt Dynapro plate reader. Finally, the protein content of purified particles was determined by microfluidic gel electrophoresis using an Agilent Bioanalyzer 2100 equipped with Series II Protein 80 chips. The relative protein content of VLPs was measures by comparing the ratios of peak integrations as displayed in the Bioanalyzer software. Particle preps routinely yielded particles bearing between 5 and 12 copies of EGF on average and yielded ~25 mg/L of culture.

Note: When purification is carried out in phosphate buffer, particle aggregates were the dominant species following sucrose gradients. Using TBS for the initial purification steps (pre-sucrose gradient) largely eliminated this problem. Purified particles resuspended in PBS did not exhibit the same aggregation behavior as the crude particles.

Bioconjugation of AlexaFluor488 to Qβ-EGF

We utilized a two-step protocol for bioconjugation; this involved standard NHS chemistry to attach an azide followed by copper-catalyzed azide-alkyne cycloaddition chemistry. First, 2 mg of Qβ-EGF or Qβ-WT (144 nmol subunits, 576 nmol lysine) dissolved in 200 μL of 1x PBS was combined with 700 μL of 0.1 M KPO_4 (pH 7.4). 100 μL of NHS-N_3 (**2**) in DMSO (3 mg/mL, 965 nmol) was slowly added to this solution and allowed to react overnight on a rotisserie. The following morning, the reaction mixtures were purified on 10-40% sucrose velocity gradients using an SW41 rotor (41K, 2.5 hours). The entire band of visible particles was collected and ultrapelleted in a 70.1 Ti rotor for at least 2 hours. The pellet was resuspended in 500 μL of 1x PBS and taken forward in its entirety for conjugation to AlexaFluor488-alkyne (**4**). The “click” conjugation proceeded as previously described. The following reagents were added in order and allowed to react on the benchtop overnight at room temperature: Qβ-EGF (500 μL), **4** (20 μL, 0.5 mM), 0.1 M KPO_4 (300 μL), $CuSO_4$ (2.5 μL, 50 mM), THPTA (12.5 μL, 50 mM), (Note: $CuSO_4$ and THPTA are pre-mixed prior to addition) aminoguanidine (25 μL, 50 mM), sodium ascorbate (25 μL, 100 mM). The reactions were purified by 10-40% sucrose velocity gradients and pelleted in a 70.1 Ti rotor as described in step one of the bioconjugation. Protein content of the final products was assessed using a Bradford assay, purity via FPLC, and size using dynamic light scattering. Control wild-type Qβ particles were conjugated in parallel using identical buffer conditions for each batch of particles made and tested. Particles were sterile filtered through a 0.2 μm syringe filter prior to use in cell-based assays.

Cell Culture

All cell culture reagents were purchased from Invitrogen, unless noted otherwise. A431 cells were a gift from the Barbas lab (Scripps, La Jolla). Cells were grown and maintained in Dulbecco’s Modified Eagle Medium (DMEM) supplemented with 10% newborn calf serum (NCS) (Omega Scientific), 1 mM sodium pyruvate, 100 units/mL penicillin, 100 μg/mL streptomycin, and 2 mM GlutaMax. Cells were grown at 37 °C in a humidified 5% CO_2 and

95% air air atmosphere. Cells used for *in vitro* experiments were used at passage numbers less than 15.

Confocal

2×10^5 A431 cells were seeded into glass bottom culture dishes (MatTek) and grown for 24 hr in complete growth media. Qβ particles were prepared in DMEM, supplemented with 1 mM sodium pyruvate and 2 mM GlutaMAX. Cells were rinsed with PBS, before the addition of Qβ particles at a final concentration 2 nM (~10^6 particles/cell). Treated cells were then incubated at 4°C or 37°C (as indicated in the text) in a humidified 5% CO_2/95% air atmosphere for 1 hr. For competition experiments, soluble EGF (2 μM) was co-incubated with the Qβ particles. After the hour incubation period, cells were rinsed twice with PBS, fixed with 2% paraformaldehyde (Electron Microscopy Sciences) in PBS for 20 min at RT, and washed again two times with PBS. Nuclei were stained with DAPI (Biotium) for 30 min at RT, washed twice with PBS, and mounted with coverslips using ImmunO-Fluore mounting media (MP Biomedicals LLC). Images were acquired on a Bio-Rad (Zeiss) Radiance 2100 Rainbow laser scanning confocal microscope equipped with a 60x oil immersion objective, and analyzed using ImageJ software.

Flow Cytometry

A431 cell monolayers were detached using Accutase (Innovative Cell Technologies, Inc.), pelleted, and resuspended in PBS. Approximately 2×10^5 cells were aliquoted into Titertube Micro Test Tubes (Bio-Rad). Qβ particles were added directly to the cell suspensions, at a final concentration of 2 or 20 nM, and incubated for 1 hr at 37°C in a humidified 5% CO_2/95% air atmosphere. Cells were then washed twice with FACS buffer (PBS, 1% NCS, 2 mM EDTA) and fixed with 1% paraformaldehyde for 10 min at RT. After two additional washings, cells were resuspended and stored in FACS buffer until analysis. Competitive binding experiments were performed by adding free EGF (0.2, 2, 20, 200, or 2000 nM) to the cell suspension, incubating at RT for 1 min, followed by the addition of Qβ-EGF particles at concentrations indicated in the text. The cells were then incubated and treated as described previously. Flow cytometric data was obtained on a Digital LSR II flow cytometer (BD Biosciences) and analyzed using FlowJo software (Tree Star Inc.).

Whole Cell ELISA

A431 cells were plated in 96-well microtiter plates in triplicate (10^4 cells/well) in 100 μL of serum free DMEM. After 24 hours media was removed and protein solutions (Qβ-EGF, EGF, or QβWT) prepared in serum-free DMEM (100 μL/well) to the indicated concentrations were added to the cells and allowed to incubate for 60 minutes at 37 °C. Following incubation with the active species, media was removed, and the whole cell ELISA proceeded per the manufacturer's recommended protocol (Thermo Fisher). Phosphorylation was detected using anti-EGFR Y1173 at a 1:500 dilution (Millipore).

Cell Viability Assays

A431 cells were plated in 96-well microtiter plates in triplicate (10^4 cells/well) in 100 μL of complete DMEM. After 18 hours, media was replaced with serum free media for 6 hours. Following serum starvation, protein solutions (Qβ-EGF, EGF, or QβWT) prepared in serum-free DMEM (100 μL/well) to the indicated concentrations were added to the cells and allowed to incubate for 72 hours at 37 °C. Cells were then assayed for viability using the MTT assay. MTT (5 mg/mL, 25 μL/well) was added to each individual well and incubated at 37 °C for approximately 1 hour (assay was stopped when significant accumulation of purple formazan crystals were visibly observed in control wells). Media was carefully aspirated and DMSO was added (200 uL/well) to dissolve the purple MTT-formazan

crystals. Absorbance of the dissolved formazan was quantified at 570 nm using a UV-Vis plate reader and cell viability was determined as a fraction of absorbance relative to untreated control wells. Data are presented as average values +/- standard deviation.

Acknowledgments

This work was supported by the National Institutes of Health (CA112075, RR021886, R21EB005364), a Pathway to Indepen-dence Award (K99EB011530) to J.K.P., and an NSF predoctoral research fellowship to M.L.H.

References

1. (a) Hilgenbrink AR, Low PS. J Pharm Sci. 2005; 94:2135. [PubMed: 16136558] (b) Shi D. Adv Funct Mater. 2009; 19:3356.(c) Whitehead KA, Langer R, Anderson DG. Nat Rev Drug Disc. 2009; 8(d) Yoo JW, Chambers E, Mitragotri S. Curr Pharm Des. 2010; 16:2298. [PubMed: 20618151] (e) Petrelli F, Borgonovo K, Barni S. Exp Opin Pharmacother. 2010; 11:1413.(f) Lee JH, Yigit MV, Mazumdar D, Lu Y. Adv Drug Deliv Rev. 2010; 62:592. [PubMed: 20338204]
2. (a) Stephanopoulos N, Tong GJ, Hsiao SC, Francis MB. ACS Nano. 2010; 4:6014. [PubMed: 20863095] (b) Banerjee D, Liu A, Voss N, Schmid S, Finn MG. ChemBioChem. 2010; 11:1273. [PubMed: 20455239]
3. (a) Kolishetti N, Dhar S, Valencia PM, Lin LQ, Karnik R, Lippard SJ, Langer R, Farokhzad OC. Proc Natl Acad Sci U S A. 2010; 107:17939. [PubMed: 20921363] (b) Zhang K, Rossin R, Hagooly A, Chen Z, Welch MJ, Wooley KL. J Polym Sci A. 2008; 46:7578.(c) Vachutinsky Y, Oba M, Miyata K, Hiki S, Kano MR, Nishiyama N, Koyama H, Miyazono K, Kataoka K. J Controlled Rel. 2011; 149:51.
4. (a) Chattopadhyay N, Cai Z, Pignol J, Keller B, Lechtman E, Bendayan R, Reilly RM. Mol Pharm. 2010; 7:2194. [PubMed: 20973534] (b) Maus L, Dick O, Bading H, Spatz JP, Fiammengo R. ACS Nano. 2010; 4:6617. [PubMed: 20939520]
5. (a) Kickhoefer VA, Garcia Y, Mikyas Y, Johansson E, Zhou JC, Raval-Fernandes S, Minoofar P, Zink JI, Dunn B, Stewart PL, Rome LH. Proc Natl Acad Sci U S A. 2005; 102:4348. [PubMed: 15753293] (b) Kickhoefer VA, Han MM, Raval-Fernandes S, Poderycki MJ, Moniz RJ, Vaccari D, Silvestry M, Stewart PL, Kelly KA, Rome LH. ACS Nano. 2009; 3:27. [PubMed: 19206245]
6. Uchida M, Kosuge H, Terashima M, Willits DA, Liepold LO, Young MJ, McConnell MV, Douglas T. ACS Nano. 2011; 5:2493. [PubMed: 21391720]
7. (a) Wan S, Coveney PV. Interface. 2011; 8:1114. [PubMed: 21227963] (b) Gondi CS, Gorantla B, Bhujanga Rao AKS, Amala K, Naidu MUR, Jogi KV, Venkat Ramana G, Myneni PC, Junnarkar A, Rao JS. Int J Oncol. 2011; 39:641. [PubMed: 21674127] (c) Lozano-Leon A, Perez-Quintela BV, Iglesias-García J, Urisarri-Ruiz A, Lariño-Noia J, Abdulkader I, Varo E, Forteza J, Domínguez-Muñoz JE. Oncol Rep. 2011:315. [PubMed: 21573507]
8. Yarden Y, Sliwkowski MX. Mol Cell Biol. 2001; 2:127.
9. Quatrale AE, Porcelli L, Silvestris G, Colucci N, Angelo A, Azzariti A. Front Biosci. 2011; 16:1962. [PubMed: 21196276]
10. (a) Quatrale AE, Petriella D, Porcelli L, Tommasi S, Silvestris N, Colucci G, Angelo A, Azzariti A. Front Biosci. 2011; 16:1973. [PubMed: 21196277] (b) Tejani MA, Cohen RB, Mehra R. Biologics. 2010; 4:173. [PubMed: 20714355]
11. (a) Shimada T, Ueda M, Jinno H, Chiba N, Wada M, Watanabe J, Ishihara K, Kitagawa Y. Anticancer Res. 2009; 29:1009. [PubMed: 19414339] (b) Yuan Q, Lee E, Yeudall WA, Yang H. Oral Oncol. 2010; 46:698. [PubMed: 20729136] (c) Sigot V, Arndt-Jovin DJ, Jovin TM. Bioconjugate Chem. 2010; 21:1465.
12. Kitai Y, Fukuda H, Enomoto T, Asakawa Y, Suzuki T, Inouye S, Handa H. J Biotechnol. 2011:1.
13. (a) Vasiljeva I, Kozlovska T, Cielens I, Strelnikova A, Kazaks A, Ose V, Pumpens P. FEBS Lett. 1998; 431:7. [PubMed: 9684855] (b) Kozlovska TM, Cielens I, Vasiljeva I, Strelnikova A, Kazaks A, Dislers A, Dreilina D, Ose V, Gusars I, Pumpens P. Intervirology. 1996; 39:9. [PubMed: 8957664] (c) Golmohammadi R, Fridborg K, Bundule M, Valegard K, Liljas L. Structure. 1996; 4:543. [PubMed: 8736553]

14. Ashcroft AE, Lago H, Macedo JMB, Horn WT, Stonehouse NJ, Stockley PG. J Nanosci Nanotechnol. 2005; 5:2034. [PubMed: 16430137]
15. (a) Domingo-Calap P, Pereira-Gómez M, Sanjuán R. J Evol Biol. 2010; 23:2453. [PubMed: 20831733] (b) Manzenrieder F, Luxenhofer R, Retzlaff M, Jordan R, Finn MG. Angew Chem Int Ed. 2011; 50:2601.
16. (a) Brown SD, Fiedler JD, Finn MG. Biochemistry. 2009; 48:11155. [PubMed: 19848414] (b) Udit AK, Brown S, Baksh MM, Finn MG. J Inorg Biochem. 2008; 102:2142. [PubMed: 18834633] (c) Udit AK, Everett C, Gale AJ, Kyle JR, Ozkan M, Finn MG. ChemBioChem. 2009; 10:503. [PubMed: 19156786]
17. Manayani D, Thomas DE, Dryden KA, Reddy V, Siladi ME, Marlett JM, Ralney GJA, Pique ME, Scobie HM, Yeager M, Young JAT, Manchester M, Schneemann A. PLoS Pathogens. 2007; 3:1422. [PubMed: 17922572]
18. Peabody DS, Manifold-Wheeler B, Medford A, Jordan SK, Caldeira JD, Chackerian B. J Mol Biol. 2008; 380:252. [PubMed: 18508079]
19. (a) Ojala K, Mottershead DG, Suokko A, Oker-Blom C. Biochem Biophys Res Commun. 2001; 284:777. [PubMed: 11396970] (b) Ojala K, Koski J, Ernst W, Grabherr R, Jones I, Oker-Blom C. Technol Cancer Res Treat. 2004; 3:77. [PubMed: 14750896] (c) Raty JK, Airenne KJ, Marttila AT, Marjomaki V, Hytonen VP, Lehtolainen P, Laitinen OH, Mahonen AJ, Kulomaa MS, Yia-Herttuala S. Mol Ther. 2004; 9:282. [PubMed: 14759812]
20. Kurata N, Shishido T, Muraoka M, Tanaka T, Ogino C, Fukuda H, Kondo A. J Biochem. 2008; 144:701. [PubMed: 18838435]
21. (a) Abdull Razis AF, Ismail EN, Hambali Z, Abdullah MNH, Ali AM, Mohd Lila MA. Appl Biochem Biotechnol. 2008; 144:249. [PubMed: 18556814] (b) Sharma K, Babu PVC, Sasidhar P, Srinivas VK, Mohan VK, Krishna E. Protein Expr Purif. 2008; 60:7. [PubMed: 18430585]
22. Richardson SM, Wheelan SJ, Yarrington RM, Boeke JD. Genome Res. 2006; 16:550. [PubMed: 16481661]
23. Fiedler JD, Brown SD, Lau J, Finn MG. Angew Chem Int Ed. 2010; 49:9648.
24. Panchuk-Voloshina N, Haugland RP, Bishop-Stewart J, Bhalgat MK, Millard PJ, Mao F, Leung WY, Haugland RP. J Histochem Cytochem. 1999; 47:1179. [PubMed: 10449539]
25. Hong V, Presolski SI, Ma C, Finn MG. Angew Chem Int Ed. 2009; 48:9879.
26. (a) Bhirde AA, Patel V, Gavard J, Zhang G, Sousa AA, Masedunskas A, Leapman RD, Weigert R, Gutkind JS, Rusling JF. ACS Nano. 2009; 3:307. [PubMed: 19236065] (b) Bohl Kullberg E, Bergstrand N, Carlsson J, Edwards K, Johnsson M, Sjöberg S, Gedda L. Bioconjugate Chem. 2002; 13:737.(c) Capala J, Barth RF, Bendayan M, Lauzon M, Adams DM, Soloway AH, Fenstermaker RA, Carlsson J. Bioconjugate Chem. 1996; 7:7.
27. Liberelle B, Boucher C, Chen J, Jolicoeur M, Durocher Y, De Crescenzo G. Bioconjugate Chem. 2010; 21:2257.
28. Ullrich A, Coussens L, Hayflick JS, Dull TJ, Gray A, Tam AW, Lee J, Yarden Y, Libermann TA, Schlessinger J. Nature. 1984; 309:418. [PubMed: 6328312]
29. Beuttler J, Rothdiener M, Müller D, Frejd FY, Kontermann RE. Bioconjugate Chem. 2009; 20:1201.
30. (a) Helin K, Beguinot L. J Biol Chem. 1991; 266:8363. [PubMed: 2022652] (b) Sorkin A, Helin K, Waters CM, Carpenter G, Beguinot L. J Biol Chem. 1992; 267:8672. [PubMed: 1314835]
31. (a) Barnes DW. J Cell Biol. 1982; 93:1. [PubMed: 7040412] (b) Gill GN, Lazar CS. Nature. 1981; 293:305. [PubMed: 6268987]
32. (a) Gulli L, Palmer K, Chen Y. Cell Growth Differen. 1996; 7:173.(b) Cao L, Yao Y, Lee V, Kiani C, Spaner D, Lin Z, Zhang Y, Adams ME, Yang BB. J Cell Biochem. 2000; 77:569. [PubMed: 10771513]

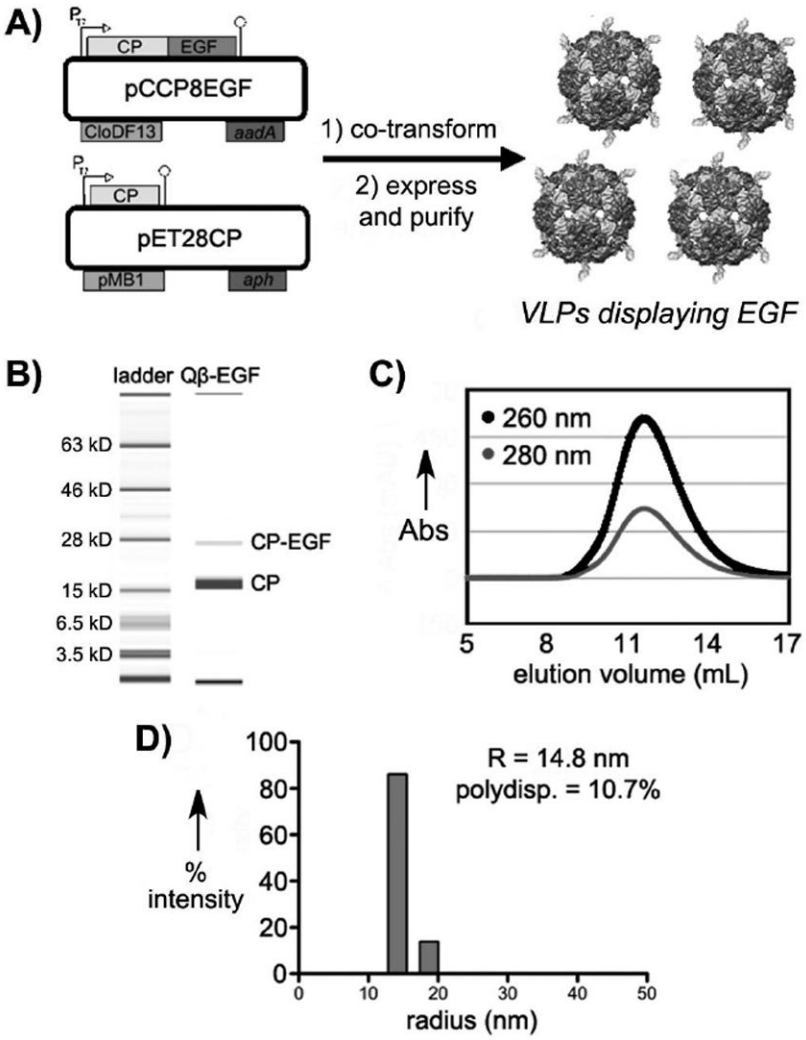

Figure 1.

Expression and characterization of EGF-displaying hybrid Qβ particles. (A) Schematic representation of plasmids used for particle production and the resulting EGF-displaying particles. (B) Electrophoretic analysis; (C) FPLC elution profile; (D) Dynamic light scattering histogram of Qβ-EGF particles.

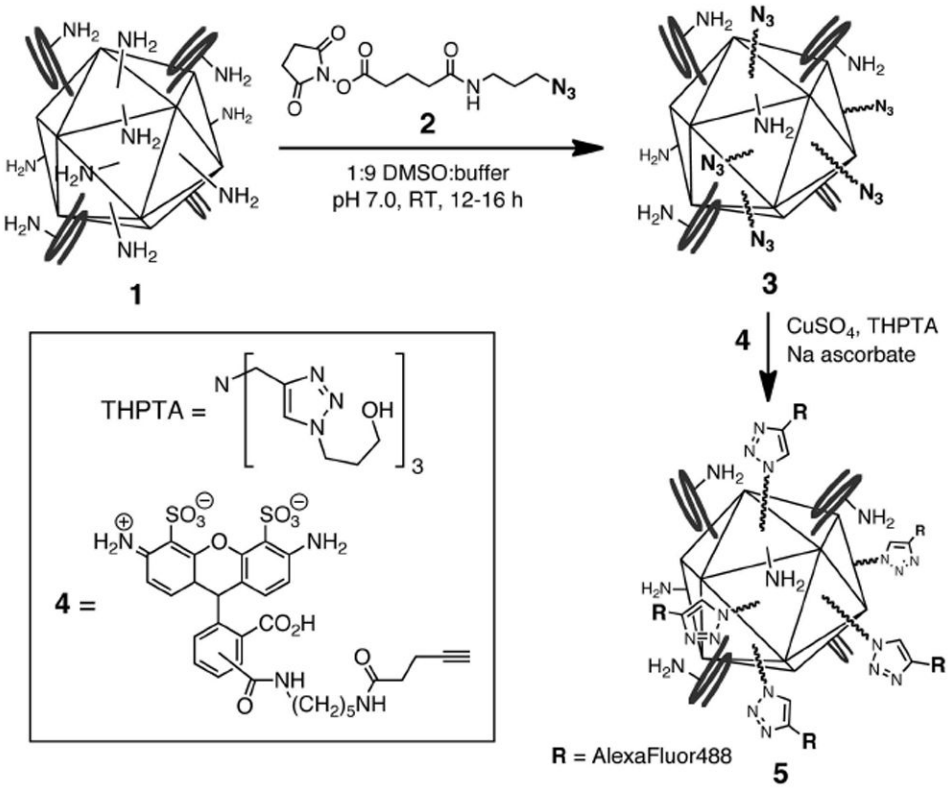

Figure 2.
Preparation of dye-labeled Qβ-EGF particles.

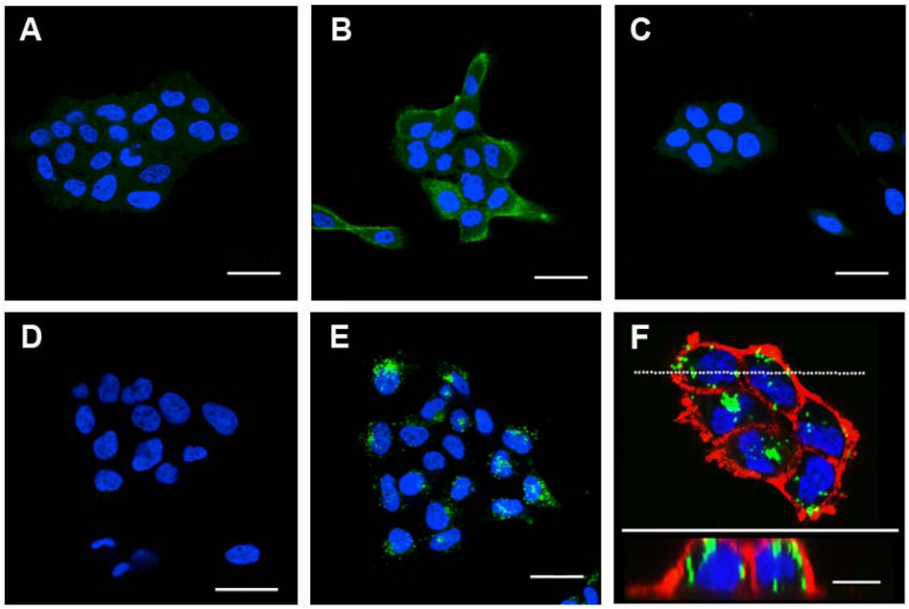

Figure 3.

Confocal fluorescence microscopy images of A431 cells treated with the following reagents (A) Qβ$(A488)_{20}$ particles (2 or 20 nM) at 4°C for 1 h. (B) Qβ$(EGF)_{11}(A488)_{20}$ particles (2 nM) at 4°C for 1 h. (C) Qβ$(EGF)_{11}(A488)_{20}$ (2 nM) in the presence of 100-fold molar excess (per displayed EGF domain) of soluble EGF at 4°C for 1 h. (D) Qβ$(A488)_{20}$ (2 or 20 nM) at 37°C for 1 h. (E) Qβ$(EGF)_{11}(A488)_{20}$ at 37°C for 1 h. (F) (top) Z-series (12.6 μm deep, step size 0.3 μm) of A431 cells treated with Qβ$(EGF)_{11}(A488)_{20}$ particles (20 nM) as in panel E; (bottom) projection of Z-series along the line shown in the top image. Blue = nuclei stained with DAPI (10 μg/mL, 30 min, 25 °C); red (panel F) = cellular membrane stained with wheat-germ agglutinin AlexaFluor555 (10 μg/mL); scale bars = 30 μm (panels A-E) or 10 μm (panel F).

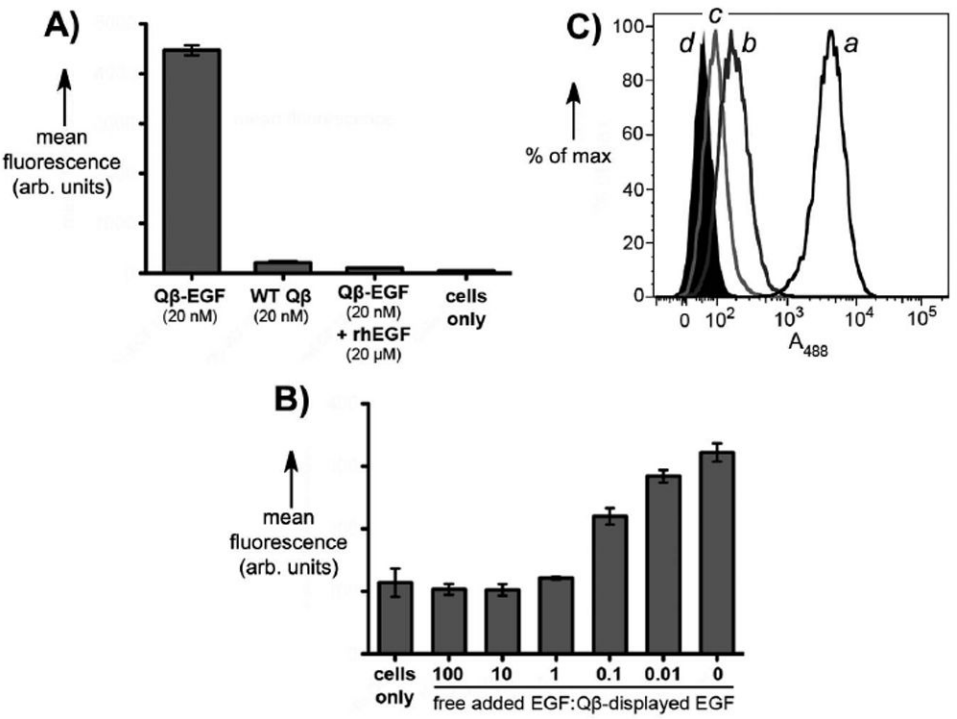

Figure 4.

Flow cytometry analyses of (A) the indicated particles binding to A431cells after 1 h incubation at 37°C. (B) Similar treatment as (A), in the presence of the indicated amount of rhEGF. $Q\beta(EGF)_{11}(A488)_{20}$ concentration was maintained at 2 nM in VLP, approximately 20nM in EGF, rhEGF concentration ranged from 2 μM (100:1) to 0.2 nM (0.01:1). (C) Representative histogram of a typical binding experiment. *a* = $Q\beta(EGF)_{11}(A488)_{20}$, *b* = $Q\beta(A488)_{20}$, *c* = $Q\beta(EGF)_{11}(A488)_{20}$ in the presence of 100-fold excess of soluble EGF, *d* = cells only. All experiments were performed in triplicate.

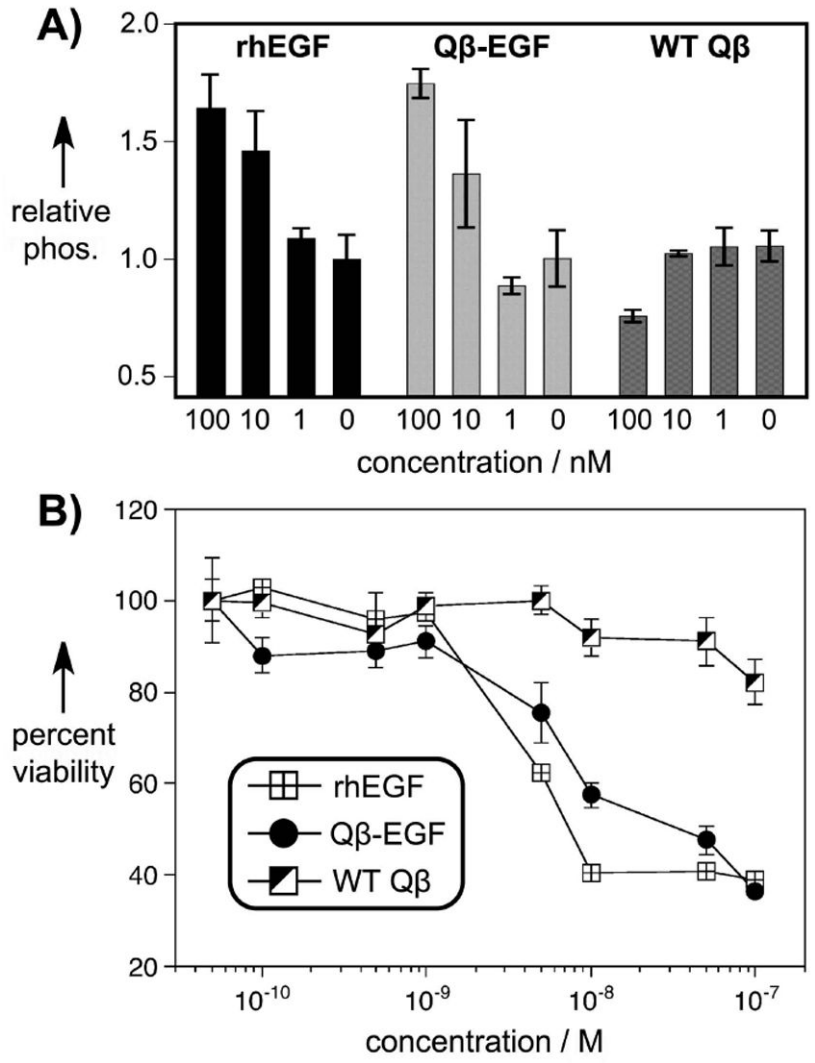

Figure 5.

(A) ELISA analysis of EGFR phosphorylation upon treatment of A431 cells with the indicated protein, relative to treatment with buffer alone. The indicated concentrations of VLP formulations are those of the particles. (B) Results of MTT assay for A431 cell viability in the presence of the indicated samples for 72 h at 37°C.